Sei-Bum Choi
Research Staff.

J. K. Hedrick
Professor.

Department of Mechanical Engineering,
University of California,
Berkeley, CA 94720

Robust Throttle Control of Automotive Engines: Theory and Experiment

An adaptive, sliding control algorithm is developed for automated throttle control of an I.C. engine to be used in drive-by-wire applications such as coordinated engine/transmission gear shiftings, traction control and autonomous vehicle control (IVHS). The paper presents a new sliding control formulation that includes combustion transport delays and a simplified adapation law to account for slowly varying engine parameters. The new technique is evaluated by computer simulation and laboratory dynamometer tests.

1 Introduction

In recent years, dynamic models for automotive engines have been developed that are accurate enough to be used for nonlinear controllers, but simple enough to be computed in real time (Moskwa and Hedrick, 1989). Previous research on automotive powertrain control has indicated that if a high performance engine controller can be combined with transmission controls on a clutch-to-clutch transmission, significantly improved shift quality can be achieved (Moskwa and Hedrick, 1990). An engine controller designed for this purpose must not only have high performance, but it must also be robust to modeling errors and be computationally efficient. Sliding controls have been shown to have very good robustness properties, but the relative degree of the system, i.e., the number of times that the system output must be differentiated before the resulting expression becomes a function of the input, can be a critical parameter in determining the complexity of the controller design (Slotine and Li, 1991). Systems with a relative degree higher than one are especially difficult since a sliding mode control derivation for such a system will require that the model be differentiated several times. The two surface scheme was developed to reduce the relative order between the input and output to one (Green and Hedrick, 1990). It is accomplished by defining intake manifold air mass (or equivalently manifold pressure and temperature) as a synthetic input to the output (engine speed), then treating that mass as a synthetic output of the actual input (throttle). Each of these two synthetic systems has a relative degree of one and the sliding surface is therefore greatly simplified.

This paper outlines the design of a multi-surface sliding mode engine control algorithm, and the derivation of adaptive algorithms to improve the performance of the controller under the presence of parametric uncertainties. The performance of the multi-surface adaptive controller will be demonstrated both through simulation and through implementation on an automotive engine.

The purpose of this study is to develop a robust throttle control algorithm for all drive-by-wire applications such as coordinated engine/transmission gear shifting, traction control and autonomous vehicle control, e.g., IVHS.

2 Engine Modeling

Engine models have been developed by many authors for a variety of purposes (Powell et al., 1981; Powell, 1987; Woods and Goh, 1979; Ohata and Ishida, 1982). Dobner (1980) developed an empirical model incorporating steady-state engine maps. Moskwa and Hedrick (1989) simplified this model for real-time engine control. A convenient version of this model for throttle control alone is the following two state version (see Table 1):

$$J_e\dot{\omega}_e = T_{net}(\omega_e, m_a) - T_L \tag{1}$$

$$P_mV = m_aT_m\bar{R} \tag{2}$$

$$\dot{m}_a = \dot{m}_{ai}(\alpha, m_a) - \dot{m}_{ao}(\omega_e, m_a) \tag{3}$$

$$\dot{m}_{ai} = \text{MAX TC}(\alpha)\ \text{PRI}(P_m/P_a) \tag{4}$$

Equation (1) is Newton's law for the engine where J_e is the "effective" engine rotational inertia and, depending upon the application, can be a function of various powertrain inertias, vehicle mass and the transmission gear ratio to reflect back to the engine (Cho and Hedrick, 1989). $T_{net}(\omega_e, m_a)$ is the net combustion torque (indicated torque minus friction torque) and is provided by the engine manufacturer as a table-look-up. T_L is the load torque on the engine and, similar to the effective engine inertia, can be dependent on engine speed, gear ratio, grade change etc. In this paper, T_L represents the dynamometer load which will be set to a constant. Equation (2) is the ideal gas law for air which we assume approximates the relationship between intake manifold pressure, temperature, and air mass. V and $\bar{R}$ are taken to be constant. Equation (3) is the flow continuity equation for the flow of air into and out of the intake manifold. $\dot{m}_{ai}$ represents the mass air flow through the throttle valve and depends upon the projected area the air flow sees as a function of throttle position (TC(α)) and the choked flow condition across the valve (PRI(P_m/P_a)). Graphical and analytical representations for these two functions are given in Cho and Hedrick (1989). $\dot{m}_{ao}$ is the mass air flow rate into the cylinders and is provided as a steady-state map as a function of ω_e and m_a.

The intake manifold dynamics (Eq. (3)) is generally faster than the engine rotational dynamics (Eq. (1)) with the possible exception of transmission gear shifting coordinations. Clearly the speed of the engine dynamics depends upon the size of J_e. For the experimental work, in this paper (engine/dyno) it was necessary to include m_a as a state. For other drive-by-wire applications it may be possible to neglect intake manifold transients and to set,

$$\dot{m}_{ai}(\alpha, m_a) = \dot{m}_{ao}(\omega_e, m_a) \tag{5}$$

It is then possible to combine the two steady-state engine maps into one, i.e.,

Contributed by the Dynamic Systems and Control Division for publication in the JOURNAL OF DYNAMIC SYSTEMS, MEASUREMENT, AND CONTROL. Manuscript received by the DSCD March 15, 1992. Associate Technical Editor: E. H. Law.

Table 1 Nomenclature

Symbol	Meaning
C_t	torque constant
J_e	effective engine inertia
m_a	mass of air in the manifold
$\dot{m}_{ai}$	mass flow of air into the manifold
$\dot{m}_{ao}$	mass flow of air out of the manifold
MAX	maximum air flow through throttle (constant)
P_m	air pressure in the manifold
P_a	atmospheric air pressure
PRI	normalized throttle flow as a function of pressure ratio (P_m/P_a)
$\bar{R}$	gas constant of air
S_1	engine speed sliding surface
S_2	intake manifold air mass sliding surface
T_L	externally applied torque
T_{net}	net engine torque
TC	normalized throttle flow as a function of throttle position
α	throttle position
ω_e	engine speed

$$T_{\text{net}} = T_{\text{net}}(\alpha, \omega_e) \tag{6}$$

which simplifies the control algorithm. We have not considered EGR (Exhaust Gas Recirculation) in this simplified model and we assume that independent controllers maintain proper spark timing and air/fuel ratio.

3 Development of a Multi-Surface Sliding Mode Controller

The sliding mode controllers discussed in this paper are based on the two state engine model developed above. At first, the throttle/torque time delay is neglected in order to design a causal controller. A controller which considers the plant time delay is discussed in the next chapter.

3.1 Algorithm Derivation. The relative degree, defined as the number of times the system output must be differentiated to get an explicit input/output relationship, between engine speed and throttle control action is two. A way to reduce the relative degree is to define one of the states to be a synthetic control (Green and Hedrick, 1990). The synthetic control is defined to be a state that, although it might not be the true input to the system, is taken to be the input for controller design. If the relative order between the synthetic control and the system output is less than the relative degree of the original system, and if the synthetic control can be made to track its reference with a boundable error, then a simple control algorithm may be designed using the synthetic control as the input. Since the relative degree of the redefined system will be reduced, the output will be differentiated fewer times, and less knowledge of the plant is necessary. Let the manifold air mass be a synthetic control, then the relative degree between engine speed and the control is one. As usual, define the first sliding surface and differentiate it:

$$S_1 \equiv \omega_e - \omega_{edes} \tag{7}$$

$$\dot{S}_1 = \dot{\omega}_e - \dot{\omega}_{edes} \equiv -\lambda_1 S_1 \tag{8}$$

By substituting the state equations:

$$T_{net}(\omega_e, m_{ades}) = J_e[\dot{\omega}_{edes} - \lambda_1 S_1] + T_L \tag{9}$$

or

$$m_{ades} = m_{ades}(T_{net}, \omega_e) \tag{10}$$

The next step is to force m_a to track m_{ades} with a boundable error. Since the relationship between the throttle position and manifold air mass is nonlinear, a sliding mode control law is used again:

$$S_2 \equiv m_a - m_{ades} \tag{11}$$

$$\dot{S}_2 = \dot{m}_a - \dot{m}_{ades} \equiv -\lambda_2 S_2 \tag{12}$$

A practical way of handling $\dot{m}_{ades}$ is to approximate it numerically. By substituting the state equations:

$$\dot{m}_{aides} = \dot{m}_{ao} + \dot{m}_{ades} - \lambda_2 S_2 \tag{13}$$

with control input:

$$\alpha = \text{TC}^{-1}\left[\frac{\dot{m}_{aides}}{\text{MAX PRI}}\right] \tag{14}$$

In addition to the benefit of simplifying the control law, we obtain a second design variable λ_2, where λ_1 and λ_2 are feedback control gains.

3.2 Modification of a Sliding Surface. For the second control surface, m_a[1] is measured to get the table value of $\dot{m}_{ao}$. But m_a includes measurement noise and $\dot{m}_{ao}$ is sensitive to the variation of m_a. A solution to this problem is filtering m_a, but filtering introduces phase lag. Another solution is to use m_{ades} instead of m_a. Let

$$\dot{m}_{ao} = \dot{m}_{ao}(\omega_e, m_a) \tag{15}$$

$$\dot{\tilde{m}}_{ao} \equiv \dot{m}_{ao}(\omega_e, m_{ades}) \tag{16}$$

and define

$$\dot{m}_{aides} \equiv \dot{\tilde{m}}_{ao} + \dot{m}_{ades} - \lambda_2 S_2 \tag{17}$$

instead of Eq. (13). Then

$$\dot{S}_2 = \dot{m}_{aides} - \dot{m}_{ao} - \dot{m}_{ades} = -\lambda_2 S_2 - (\dot{m}_{ao} - \dot{\tilde{m}}_{ao}) \tag{18}$$

or

$$S_2\dot{S}_2 = -\lambda_2 S_2^2 - (\dot{m}_{ao} - \dot{\tilde{m}}_{ao})S_2 \tag{19}$$

Since the air flow rate out of the manifold ($\dot{m}_{ao}$) increases as the air pressure of the manifold (m_a) increases for I.C. engines at a given speed, the partial derivative of $\dot{m}_{ao}$ with respect to m_a is greater than zero. If $S_2 > 0$, i.e., $m_a > m_{ades}$ then $\dot{m}_{ao} > \dot{\tilde{m}}_{ao}$ and vice versa. So, $(\dot{m}_{ao} - \dot{\tilde{m}}_{ao})S_2 > 0$, and this term makes the control algorithm more stable.

3.3 Discussion and Simulation Results. The engine was simulated as having a known applied load, no modeling error and no time delay. For this paper λ_1 and λ_2 were set to 10 [s^{-1}] and 80 [s^{-1}] on the basis of computer simulations. The desired trajectories for these simulations were chosen to be a sine wave and a step function. Figures 1 and 2 show that the performance of the sliding mode control algorithm is very good for a wide range of driving conditions. For simulation and experimental work T_L was set to be a constant of 67.7 N-m.

4 Time Delay Model

The total throttle/torque time delay is a combination of fueling delay and transport delay. The fueling delay depends greatly on the particular fueling method, and the transport delay is a function of the injector firing interval and the injector solenoid size as well as the engine speed (Cho and Hedrick, 1989). Combined with the lag due to filtering measured data, the total time delay is up to 70 ms at the nominal speed of 3000 rpm for the engine of this study. This time delay causes a phase shift and overshoot to the response as shown in Fig. 3. Let the

[1] The pressure and temperature are measured and the ideal gas law is used to estimate the air mass.

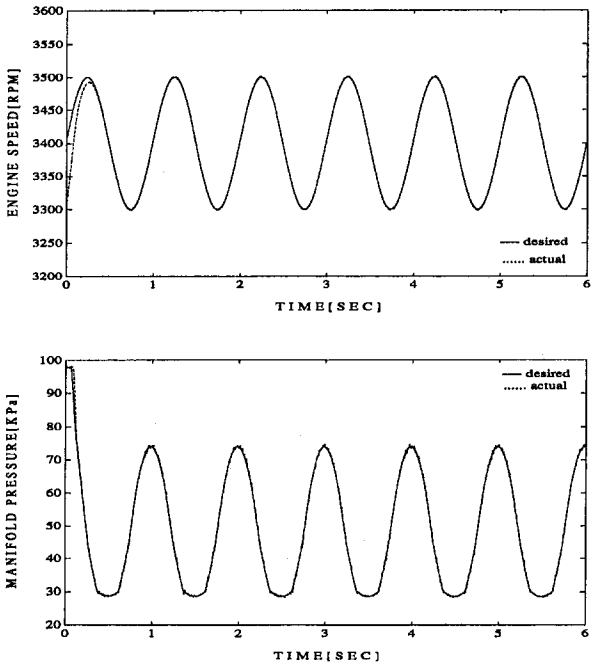

Fig. 1 Sliding control: 1 Hz, simulation

total input/output time delay be t_d, then we need to advance T_{net} by t_d as follows:

$$T_{netdes}(t) = J_e[\dot{\omega}_{edes}(t + t_d) - \lambda_1[\omega_e(t + t_d) - \omega_{edes}(t + t_d)]] + T_L \quad (20)$$

Let h be the sampling time and $t_d = nh$. If ω_{edes} is smooth enough, and ω_e and ω_{edes} satisfy the Lipschitz condition, then $\omega_{edes}(t + t_d)$ can be approximated using past data within $O(h)$:

$$T_{net} = J_e[\dot{\omega}_{edes} - \lambda_1(\hat{\omega}_e - \hat{\omega}_{edes})] + T_L + O(h) \quad (21)$$

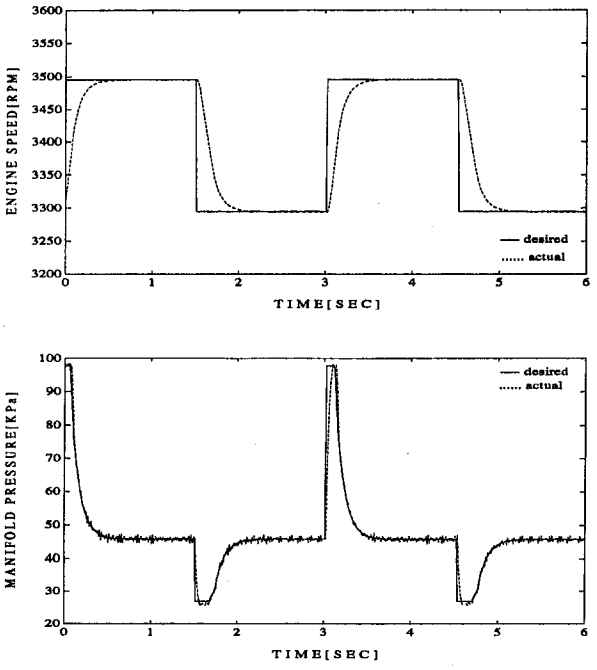

Fig. 2 Sliding control: step, simulation

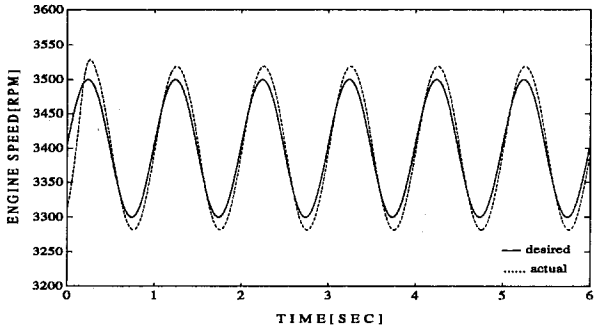

Fig. 3 Actual plant with time delay, simulation

where

$$\dot{\omega}_{edes}(t + nh) = \dot{\omega}_{edes}(t) + n[\dot{\omega}_{edes}(t) - \dot{\omega}_{edes}(t - h)] + \frac{n^2}{2}[\dot{\omega}_{edes}(t) - 2\dot{\omega}_{edes}(t - h) + \dot{\omega}_{edes}(t - 2h)] \quad (22)$$

$$\hat{\omega}_e(t + nh) - \hat{\omega}_{edes}(t + nh) = \omega_e(t) - \omega_{edes}(t) \quad (23)$$

It is not recommended to take higher order terms in Eq. (23), because this would require numerical differentiation of the measured data ω_e. For the actual plant:

$$J_e\dot{\omega}_e(t) = T_{net}(t - t_d) - T_L \quad (24)$$

With the input advanced by t_d:

$$T_{netdes}(t - t_d) = J_e[\dot{\omega}_{edes}(t) - \lambda_1[\omega_e(t) - \omega_{edes}(t)]] + T_L + O(h) \quad (25)$$

Combining Eqs. (24) and (25)

$$\dot{S}_1 = -\lambda_1 S_1 + O(h)/J_e \quad (26)$$

Thus, this time advanced control law is stable for $|S_1|$ greater than $|O(h)/(\lambda_1 J_e)|$. Figure 4 is the plot of the response of the actual plant with time delay when the input signal is advanced by t_d.

5 Parameter Adaptation

There are two values that we treated as constants that would tend to vary slowly over time. With a proper adaptive algorithm, we can use these values to improve the robustness to unusual disturbances and modeling errors. We will outline the derivation and implementation of two adaptive algorithms.

5.1 Algorithm Derivation

C_t Adaptation. The engine net torque, T_{net}, varies from engine to engine and also with time for a given engine. Let C_t be an unknown constant and:

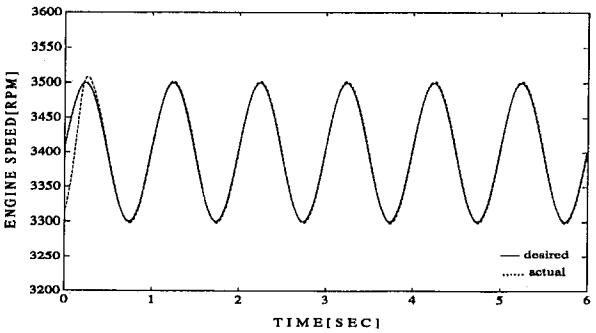

Fig. 4 Actual plant: time delay is considered, simulation

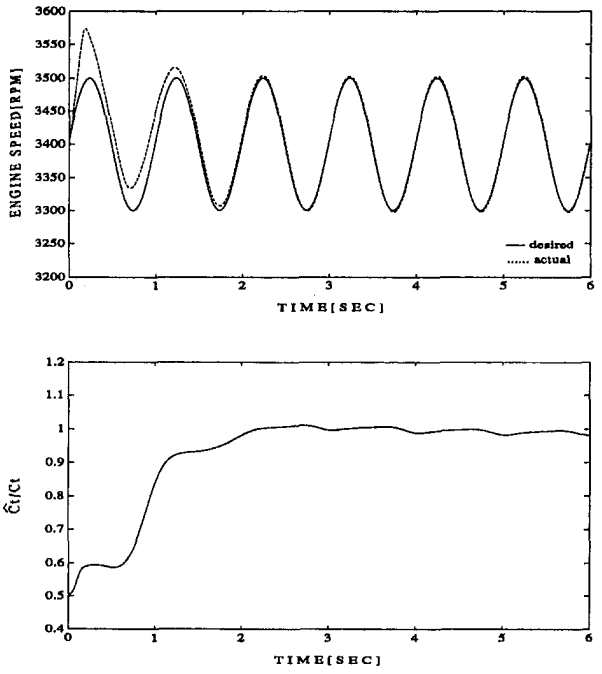

Fig. 5 Parameter adaptation: $\hat{C}_t$, simulation

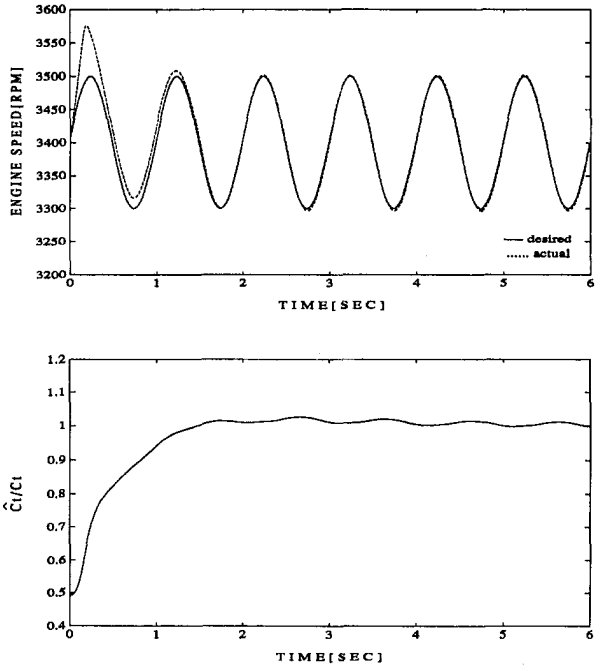

Fig. 7 Parameter adaptation: modified scheme, $\hat{C}_t$, simulation

$$T_{net} = C_t T'_{net} = J_e \dot{\omega}_e + T_L \tag{27}$$

$$T_{netdes} = \hat{C}_t T'_{net} = J_e(\dot{\omega}_{edes} - \lambda_1 S_1) + T_L \tag{28}$$

Defining $\tilde{C}_t = C_t - \hat{C}_t$, we can substitute Eq. (27) into Eq. (28) and arrive at:

$$\dot{S}_1 = \frac{\tilde{C}_t}{\hat{C}_t}\dot{\omega}_{edes} - \left(1 + \frac{\tilde{C}_t}{\hat{C}_t}\right)\lambda_1 S_1 + \frac{\tilde{C}_t}{\hat{C}_t}\frac{T_L}{J_e} \tag{29}$$

The next step is to define a Lyapunov function candidate. Let

$$V_1 \equiv \frac{1}{2}\left(S_1^2 + \frac{1}{a_1}\tilde{C}_t^2\right) \tag{30}$$

Differentiating:

$$\dot{V}_1 = S_1\dot{S}_1 - \frac{1}{a_1}\tilde{C}_t\dot{\hat{C}}_t$$

$$= -\lambda_1 S_1^2 + \tilde{C}_t\left[\frac{S_1}{\hat{C}_t}\left(\dot{\omega}_{edes} - \lambda_1 S_1 + \frac{T_L}{J_e}\right) - \frac{1}{a_1}\dot{\hat{C}}_t\right] \tag{31}$$

The first term is guaranteed to be negative and the term in the

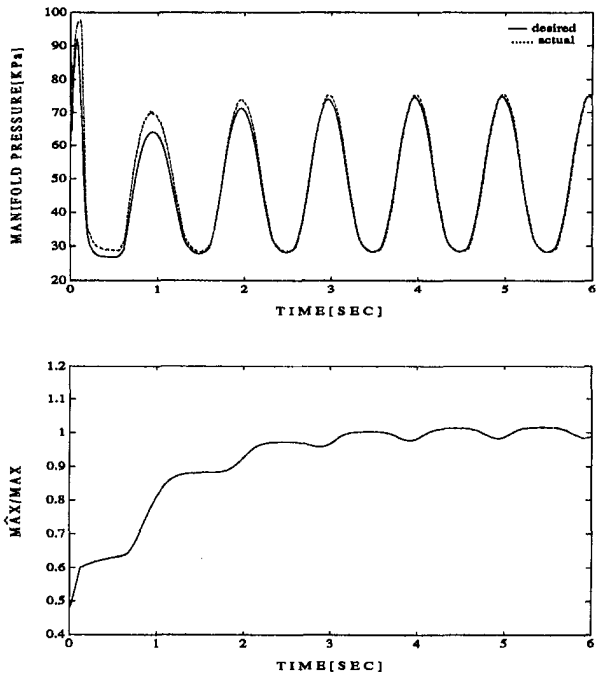

Fig. 6 Parameter adaptation: *MÂX*, simulation

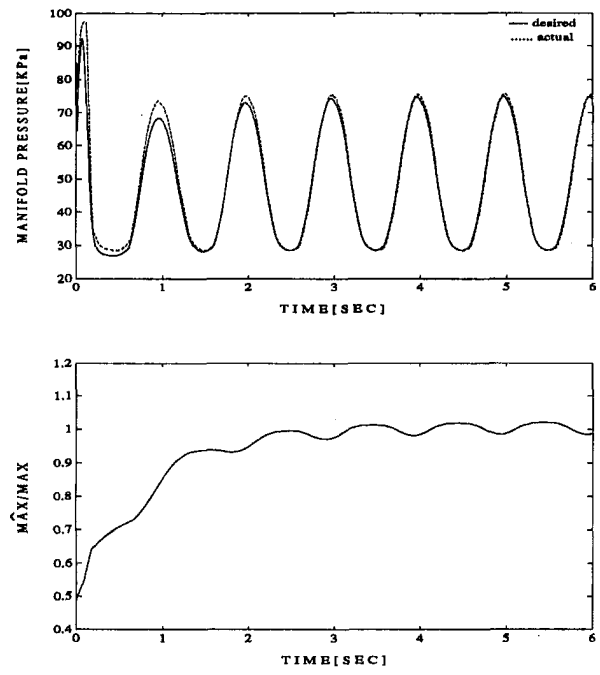

Fig. 8 Parameter adaptation: modified scheme, *MÂX*, simulation

brackets can be set to zero by the choice of $\dot{\hat{C}}_t$ thus giving a stabilizing adaptive law:

$$\dot{\hat{C}}_t = \frac{a_1 S_1}{\hat{C}_t}\left(\dot{\omega}_{edes} - \lambda_1 S_1 + \frac{T_L}{J_e}\right) \tag{32}$$

With the adaptive law given above, the derivative of the Lyapunov function is negative semi-definite. This means that S_1 will approach zero and $\hat{C}_t$ will remain bounded. Figure 5 shows the response of the adaptive controller.

MAX Adaptation. MAX which was defined as the maximum amount of air that can pass through the throttle body is a function of the ambient temperature and pressure. One way to update MAX would be to place two additional sensors on the vehicle and occasionally change the parameter. Another solution is parameter adaptation. The adaptation algorithm follows preceeding derivation. Let

$$(\dot{m}_{aides} - \dot{m}_{ao}) - \dot{m}_{ades} = -\lambda_2 S_2 \tag{33}$$

$$\dot{m}_{aides} = \hat{\text{MAX}}\ \text{PRI TC} \tag{34}$$

Defining $\tilde{\text{MAX}} = \text{MAX} - \hat{\text{MAX}}$, we can combine Eqs. (4), (33), and (34), and arrive at:

$$\begin{aligned}\dot{S}_2 &= (\dot{m}_{ai} - \dot{m}_{ao}) - \dot{m}_{ades} \\ &= (\dot{m}_{aides} - \dot{m}_{ao} - \dot{m}_{ades})\frac{\tilde{\text{MAX}}}{\hat{\text{MAX}}}\dot{m}_{aides} \\ &= -\lambda_2 S_2 + \frac{\tilde{\text{MAX}}}{\hat{\text{MAX}}}\dot{m}_{aides}\end{aligned} \tag{35}$$

The next step is to define a Lyapunov function. Let

$$V_2 \equiv \frac{1}{2}\left(S_2^2 + \frac{1}{a_2}\tilde{\text{MAX}}^2\right) \tag{36}$$

Differentiating:

$$\begin{aligned}\dot{V}_2 &= S_2\dot{S}_2 - \frac{1}{a_2}\tilde{\text{MAX}}\,\dot{\hat{\text{MAX}}} \\ &= -\lambda_2 S_2^2 + \tilde{\text{MAX}}\left[\frac{1}{\hat{\text{MAX}}}\dot{m}_{aides}S_2 - \frac{1}{a_2}\dot{\hat{\text{MAX}}}\right]\end{aligned} \tag{37}$$

The first term is guaranteed to be negative and the term in the brackets can be set to zero by the choice of $\dot{\hat{\text{MAX}}}$ which gives our adaptive law.

$$\dot{\hat{\text{MAX}}} = \frac{a_2 S_2}{\hat{\text{MAX}}}\dot{m}_{aides} \tag{38}$$

This adaptive law again guarantees that the sliding surface will be driven to zero and that $\hat{\text{MAX}}$ will be bounded. Figure 6 shows the response of the adaptive controller.

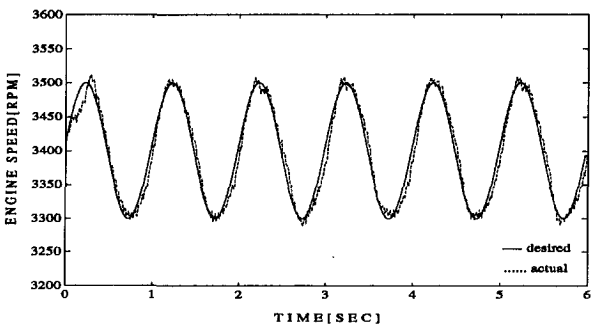

Fig. 9 Sliding control of an actual engine: 1 Hz, experiment

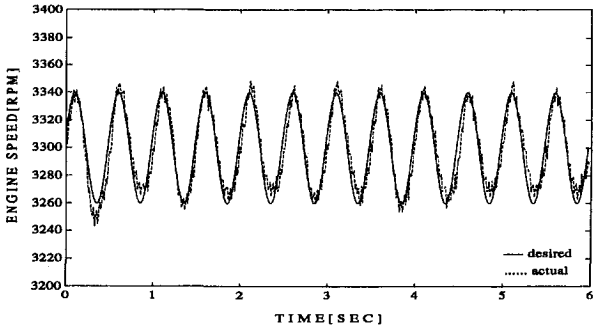

Fig. 10 Sliding control of an actual engine: 2 Hz, experiment

5.2 Modification of Adaptation Law. In Section 5.1 two adaptive laws are derived from Lyapunov functions. An easier algorithm to be implemented can be derived by relaxing the Lyapunov condition. If the relaxed Lyapunov condition is satisfied then the equilibrium point is still stable (see Appendix).

Theorem. If, around the equilibrium point 0 of a system $\dot{x} = f(x, t)$, f is continuous, bounded and there exists a scalar function $V(x, t)$ with bounded partial derivatives such that

1. $V(x, t)$ is positive definite
2. $V(x, t)$ is decrescent
3. $\dot{V}(x, t)$ is negative definite in the sense of the average

then the equilibrium point 0 is globally uniformly asymptotically stable.

By applying this condition two adaptive laws are derived which are stable and simple to implement.

C_t Adaptation. Define $\dot{\hat{C}}_t \equiv a_1 S_1 T_L/\hat{C}_t J_e \equiv \beta_1 S_1/\hat{C}_t$ then for the Lyapunov function of Eq. (30):

$$\dot{V}_1 = -\lambda_1\left(1 + \frac{\tilde{C}_t}{\hat{C}_t}\right)S_1^2 + \frac{\tilde{C}_t}{\hat{C}_t}S_1\dot{\omega}_{edes} \tag{39}$$

Let the adaptive gain β_1 be very small then $\tilde{C}_t$ may change very slowly. In addition, the degree of correlation between S_1 and $\dot{\omega}_{edes}$ is very small for small $\tilde{C}_t$ (see Eq. (29)), and $\dot{\omega}_{edes\,\Delta t} = 0$ for bounded ω_{edes} and large Δt. So,

$$\bar{\dot{V}} = -\lambda_1\left(1 + \frac{\tilde{C}_t}{\hat{C}_t}\right)S_1^2 < 0 \tag{40}$$

for small $\tilde{C}_t$. So, $\dot{\hat{C}}_t = \beta_1 S_1/\hat{C}_t$ is a possible candidate for the stabilizing adaptive law. The response of this adaptive controller is shown in Fig. 7.

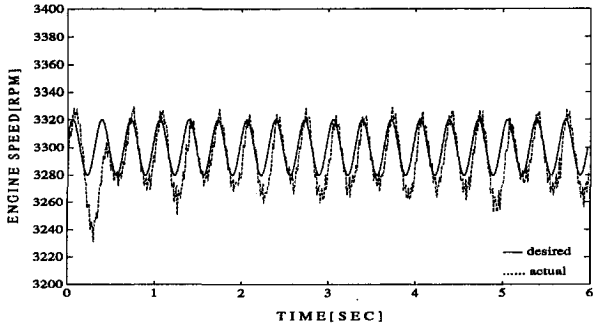

Fig. 11 Sliding control of an actual engine: 3 Hz, experiment

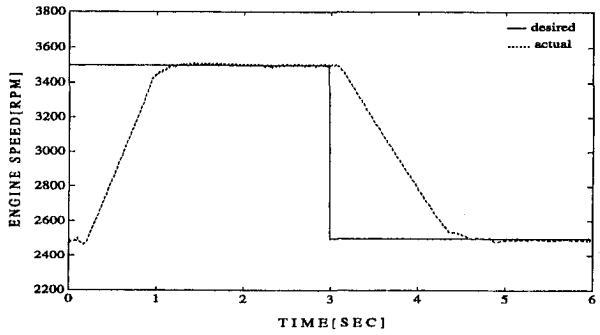

Fig. 12 Sliding control of an actual engine: step, experiment

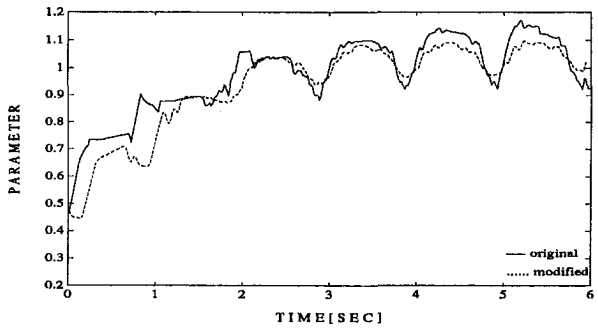

Fig. 14 Parameter adaptation: $\hat{MAX}$, experiment

MAX Adaptation. In the same manner, let $\dot{\hat{MAX}} \equiv a_2\bar{m}_{aides}S_2/\hat{MAX} \equiv \beta_2 S_2/\hat{MAX}$, then for the Lyapunov function of Eq. (36):

$$\dot{V}_2 = -\lambda_2 S_2^2 + \dot{\hat{MAX}}\frac{S_2}{\hat{MAX}}(\dot{m}_{aides} - \overline{\dot{m}_{aides}}) \quad (41)$$

Similarly,

$$\dot{\overline{V}}_2 = -\lambda_2\overline{S_2^2} + \frac{1}{\hat{MAX}}\overline{\dot{\hat{MAX}}\,S_2}(\overline{\dot{m}_{aides}} - \overline{\dot{m}_{aides}}) = -\lambda_2\overline{S_2^2} \quad (42)$$

So, $\hat{MAX} = \beta_2 S_2/\hat{MAX}$ is a stabilizing adaptive control law. Figure 8 shows the response of this adaptive controller.

5.3 Discussion. Both the original and the modified adaptive algorithms work very well in simulation. However, the responses of the modefied adaptive controllers are smoother than those of the original controllers, and stay smooth even when the adaptive gains become very large. This is reasonable when we consider that the modified adaptation algorithm is derived from a condition which satisfies the Lyapunov condition in the sense of the average.

6 Experimental Verification

The experimental verification has been made on a test stand consisting of a six cylinder 3.8 liter engine connected to a motoring dynamometer. The sliding controls have been implemented on a 16 bit, 12 MHz microcontroller running at a 12 ms loop speed. The controller senses the following engine variables: engine speed, throttle body air flow, intake manifold pressure and temperature, and throttle position. A stepper motor has been mounted directly to the throttle which allows up to 900 degrees per second of rotation with a step size of 0.9 degrees. Since small amounts of noise on the engine speed signal were amplified into an unacceptable high level of noise on the desired throttle position, first order digital filters were placed on the speed signal and the desired manifold air mass which largely eliminated the noise problem. The time constants for the equivalent analog filters are 0.02 [s] for both of them. The experimental results are for the control gains λ_1 and λ_2 set to 10 [s^{-1}] and 80 [s^{-1}] and the dynamometer load set to 67.7 [N-m].

Figures 9–12 show the actual run of a multi-surface sliding controller on the test stand when the time delay is modelled and there are no parametric uncertainties. Figures 13 and 14 compare the performance of the original and the suggested adaptive schemes tested for the same 1 Hz sinusoidal desired speed profiles as in Fig. 9.

The experimental results show that the multi-surface sliding mode controller works well up to a 3 Hz input signal with the tracking errors less than 20 rpm, which is the noise level of the speed sensor used for the test. The modified adaptive control scheme is dominant especially in the case of C_t adaptation (see Fig. 13).

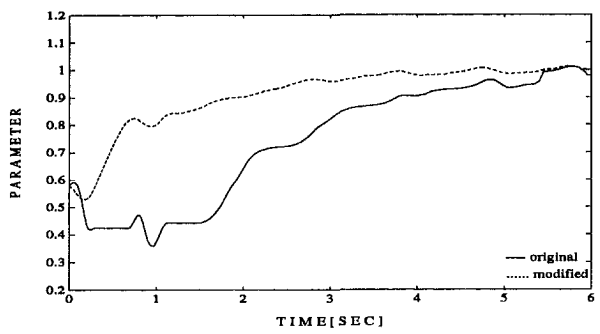

Fig. 13 Parameter adaptation: $\hat{C}_t$, experiment

7 Conclusions

New sliding mode control algorithms were derived which consider plant time delay and are robust to parametric uncertainty and measurement noise. The derived adaptive algorithms were compared by both a computer simulation and an actual engine run on a test bench. The performance of the sliding mode control algorithm is very good for a wide range of driving conditions and the adaptation algorithms are stable for 50 percent parametric uncertainties. The performance of the modified adaptive algorithms were superior especially in the experiment where modeling and sensing errors exist.

References

Cho, D., and Hedrick, J. K., 1989, "Automotive Powertrain Modeling for Control," ASME JOURNAL OF DYNAMIC SYSTEMS, MEASUREMENT, AND CONTROL, Vol. 111, Dec., pp. 568–576.

Choi, S-B., and Hedrick, J. K., 1992, "Experimental Implementation of Sliding Controls on Automotive Engines," *Proc. ACC.*

Dobner, D. J., 1980, "A Mathematical Engine Model for Development of Dynamic Engine Control," SAE Report No. 800054.

Green, J., and Hedrick, J. K., 1990, "Nonlinear Speed Control for Automotive Engine," *Proc. ACC,* Vol. 3.

Moskwa, J. J., 1988, "Automotive Engine Modeling for Real Time Control," Ph.D. Thesis, MIT.

Moskwa, J. J., and Hedrick, J. K., 1989, "Modeling and Validation of Automotive Engines for Control Algorithm Development," ASME WAM, Advanced Automotive Technologies—DSC—Vol. 13, Ed. Karmel, A. M., et al.

Moskwa, J. J., and Hedrick, J. K., 1990, "Nonlinear Algorithms for Automotive Engine Control," IEEE Control Systems Magazine, Apr.

Nesbit, C., and Hedrick, J. K., 1991, "Adaptive Engine Control," *Proc. ACC,* Vol. 2.

Ohata, A., and Ishida, Y., 1982, "Dynamic Inlet Pressure and Volumetric Efficiency of a Four Cycle Four Cylinder Engine," SAE paper No. 820407.

Powell, B. K., Wu, H., and Aquino, C. F., 1981, "Stoichiometric Air-Fuel Ratio Control Analysis," SAE paper No. 810274.

Powell, J. D., 1987, "A Review of I. C. Engine Models for Control System Design," *Proc. IFAC,* Munich.

Sastry, S., and Bodson, M., 1989, *Adaptive Control,* Prentice-Hall.

Slotine, J-J. E., and Li, W., 1991, "Applied Nonlinear Control," Prentice-Hall.

Woods, W. A., and Goh, G. K., 1979, "Compressible Flow Through a Butterfly Throttle Valve in a Pipe," *Proc. Inst. of Mech. Eng.,* Vol. 193.

APPENDIX

Derivation of an Averaging Lyapunov Condition

Define:

$$\bar{g}(x(t), t)_{\Delta t} \equiv \frac{1}{\Delta t}\int_{t}^{t+\Delta t} g(x(\tau), \tau)d\tau$$

then

$$V(x(t + \Delta t), t + \Delta t) = V(x, t) + \bar{\dot{V}}(x, t)_{\Delta t}\Delta t$$

Definition

If the function $V(x, t)$ has continuous partial derivatives, and there exists finite and positive Δt for all t such that $\bar{\dot{V}}(x, t)_{\Delta t} \leq -\gamma(\|x\|)\Delta t < 0$ then $\dot{V}$ is said to be negative definite in the Sense of Average. Where the derivative and the averages are taken along the trajectories of a system $\dot{x} = f(x, t)$, and γ is a class KR function.

Proof:

Let $t_{i+1} = t_i + \Delta t_i$'s such that $\bar{\dot{V}}(x, t_i)_{\Delta t_i} \leq -\overline{\gamma(\|x\|)}_{\Delta t_i}$. From the conditions 1 and 2 of the Theorem in section 5.2, $\alpha(\|x(t)\|) \leq V(x(t), t) \leq \beta(\|x(t)\|)$, and α and β are class KR functions. For any $R > 0$, there exists $r(R)$ such that $\beta(r) < \alpha(R)$. Let the initial condition $x(t_0)$ be chosen such that $\|x(t_0)\| < r$ then, for all $t_i > t_0$, $\alpha(R) > \beta(r) \geq V[x(t_0), t_0] \geq V[x(t_i), t_i] \geq \alpha(\|x(t_i)\|)$. So we can find $x(t_i)$'s such that $\|x(t_i)\| < R$. Since Δt_i and $\|\dot{x}\|$ are bounded, finite M_1 and M_2 can be found such that $\|x(t)\| < M_1R + M_2\sqrt{R} \equiv R'(R)$ for all $t > t_0$. If R does not go to 0 then, $\overline{\|x(t_i)\|}_{\Delta t_i}$ does not converge to 0 and there exists $a > 0$ such that for all $t_i > t_0$, $-\bar{\dot{V}}[x(t_i), t_i]_{\Delta t_i} \geq a > 0$ or

$$V[x(t_i), t_i] = V[x(t_0), t_0] + \int_{t_0}^{t_i} \dot{V}\,dt \leq V[x(t_0), t_0] - (t_i - t_0)a$$

which leads to a contradiction for large t_i. So $\overline{\|x(t_i)\|}_{\Delta t_i}$ goes to 0. But $\|x(t)\| \geq 0$ and $\|\dot{x}(t)\|$ is bounded, so $\|x(t)\|$ goes to 0 for all large enough t.